

Fusion Segmentation Algorithm for SAR images based on the Persistence and Clustering in the Contourlet Domain

Yan Wu,

*School of Electronics Engineering,
Xidian Univ.,*

Xi'an 710071, China

Haitao Zong, Xin Wang,

*School of Electronics Engineering,
Xidian Univ.,*

Xi'an 710071, China

Ping Xiao

*Shaanxi Bureau of Surveying & Mapping,
Xi'an 710054, China*

Ming Li

*National Key Lab. of Radar Signal Processing,
Xidian Univ.,*

Xi'an 710071, China

Abstract—In view of the speckle noise in the SAR images, utilizing the Contourlet's advantages of multiscale, localization, directionality and anisotropy, a new SAR image fusion segmentation algorithm based on the persistence and clustering in the Contourlet domain is proposed in this paper. The algorithm captures the persistence and clustering of the Contourlet transform, which is modeled by HMT and MRF, respectively. Then, these two models are fused by fuzzy logic, resulting in a Contourlet domain HMT-MRF fusion model. Finally, we deduce the maximum a posteriori (MAP) segmentation equation for the new fusion model. The algorithm is used to segment the real SAR images. Experimental results and analysis indicate that the proposed algorithm effectively reduces the influence of multiplicative speckle noise, improves the segmentation accuracy and provides a better visual quality for SAR images over the algorithms based on HMT-MRF in the wavelet domain, HMT and MRF in the Contourlet domain, respectively.

Keywords— SAR images segmentation; Contourlet transform; Persistence; Clustering; Fuzzy logic fusion.

I. INTRODUCTION

The segmentation of synthetic aperture radar (SAR) images is a key step in the automatic analysis and interpretation of data, which can provide the overall structural information on the image to reveal the essence of SAR images. Image segmentation establishes the foundation for automatic targets recognition (ATR) and promotes the wide application of SAR images. This domain has become a hotspot at home and abroad in recent years. Real SAR images are corrupted with an inherent signal-dependent phenomenon named multiplicative speckle noise, which is grainy in appearance and due primarily to the phase fluctuations of the electromagnetic return signals. Hence, the classical segmentation techniques that work successfully on natural images do not perform well on SAR images. Recent developments in the statistic theory have opened new avenues for nonstationary image modeling and speckle reduction^[1-3]. As a kind of pair random model, hidden Markov model (HMM) provides another method to deal with the nonstationary signal, and it can better describe the global nonstationarity and the local stationarity of signals, and so it is very suitable to dealing with nongaussian and nonsationary SAR images, and receives a wide attention. Venkatachalam and Hyeokho Choi proposed the image

segmentation algorithm based multiscale hidden Markov tree (HMT)^[4-5] model in 1998 and 2001, respectively, and applied it to SAR images segmentation. This algorithm applies the persistence property of wavelet coefficients to segmentation, and reduce the misclassification, which has a certain effect on the segmentation of SAR images. Unfortunately, the method based on HMT does not take the clustering property of wavelet coefficients into account, which leads easily to directional edge vagueness and singularity diffusion in SAR images. Because the multiplicative speckle noise in SAR images often produces a sudden change in the pixel value, and the local dependence of the image leads to pixel category having a certain relation with its neighbors' category. The Markov random field (MRF), which incorporates the spatial dependence among pixels into segmentation, can exactly reflect the clustering property of wavelet coefficients, and can use the neighborhood dependency to reduce the effect of speckle noise. Therefore MRF is used in the segmentation of SAR images^[6-9], and the segmentation result is encouraging.

For the complicated SAR images data, it is difficult to deal with SAR speckle reduction and feature extraction in the traditional wavelet sense, so we must construct a new sparse representation for the image which can efficiently extract the directional information reflecting multiscale, multiresolution and multisubband of objects, which is a key step to realize the segmentation and understanding of real SAR images. In 2002, M.N.Do and Martin Vetterli^[10-12] pioneered a sparse representation for two-dimensional piecewise smooth signals named the Contourlet transform which can capture the intrinsic geometrical structures that are key features of visual information. 2-D wavelets obtained by a tensor-product of one-dimensional wavelets only provide three directional components, lack directionality and are only good at catching point discontinuities. The Contourlet transform can efficiently capture the smooth contours and geometrical structures in the image. Contourlet not only possesses the main features of the wavelet, namely, multiresolution and time-frequency localization, but also shows a high degree of directionality and anisotropy. Based on the analysis above, HMT is extended to the Contourlet domain^[13], and thus Contourlet domain HMT efficiently captures high-dimensional singularities of the image in SAR images segmentation, and obtains a better segmentation result than HMT performed in the wavelet domain. However, the algorithm based HMT does not

consider the clustering property of Contourlet coefficients, and can not remove the effect of speckle noise completely. The Markov random field with hidden states which take the intrascale dependencies between pixels into account can effectively consider the clustering property of Contourlet coefficients, and can suppress speckle noise, but its disadvantage is that it only notices the local dependencies, and does not take the global persistence into consideration during image segmentation.

Because Contourlet can effectively capture high-dimensional singularities, we fuse HMT with MRF in the Contourlet domain by the fuzzy logic fusion approach, so the algorithm can effectively capture persistence and clustering property of Contourlet subbands, and largely reduce the influence of multiplicative speckle noise on the segmentation. We apply it to the segmentation of Synthesis texture images and real SAR images. Numerical and experimental results demonstrate the good performance of the proposed algorithm.

II. CONTOURLET TRANSFORM AND ITS COEFFICIENTS STATISTIC ANALYSIS

Contoulet transform has an elongated support of flexible aspect ratios, which is a double filter bank structure. In the double filter bank, the Laplacian pyramid (LP) is first used to capture the point discontinuities, and then a directional filter bank (DFB) links point discontinuities into linear structures. By the Contourlet transform, one can decompose each scale into any arbitrary power of two's number of directions, and different scales can be decomposed into different numbers of directions. These features make Contourlet a unique transform that can achieve a high level of flexibility in decomposition and a rigid sampling.

Fig.2 (a) plots the histograms of the finest subbands of the image Fig.1 (a). It implies that the Contourlet transform is sparse and the subband marginal distributions of natural images in the Contourlet domain are highly non-Gaussian but conditional-Gaussian. In other words, the Contourlet coefficients of natural image can be accurately modeled by a mixture of Gaussian distributions, as shown in Fig.2 (b). Fig.3 shows the conditional distributions of Contourlet coefficients, conditioned on their parents (PX) and neighbors (NX). we conclude that the Contoulet coefficients have dependencies between neighborhood and adjacent scales, which are clustering and persistence.



Fig.1 Sketch of Contourlet transform: (a) test image; (b) Contourlet transform of two scale.

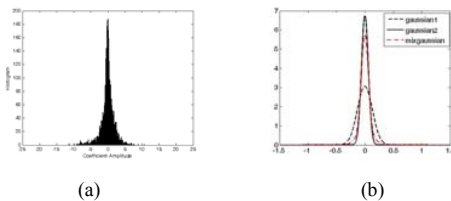


Fig.2 Marginal probability distributions of Contourlet coefficients: (a) marginal probability distribution of Contourlet decomposition subband; (b) mixture Gaussian probability density distribution.

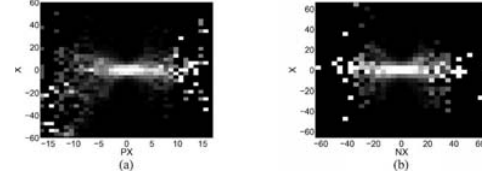


Fig.3 Conditional distribution of Contourlet coefficients in one subband: (a) $P(X|PX)$; (b) $P(X|NX)$.

Fig.2 (a) plots the histograms of the finest subbands of the image Fig.1 (a). It implies that the Contourlet transform is sparse and the subband marginal distributions of natural images in the Contourlet domain are highly non-Gaussian but conditional-Gaussian. In other words, the Contourlet coefficients of natural image can be accurately modeled by a mixture of Gaussian distributions, as shown in Fig.2 (b). Fig.3 shows the conditional distributions of Contourlet coefficients, conditioned on their parents (PX) and neighbors (NX). we conclude that the Contoulet coefficients have dependencies between neighborhood and adjacent scales, which are clustering and persistence.

III. THE HMT-MRF FUZZY FUSION SEGMENTATION IN THE CONTOURLET DOMAIN

The method based on the HMT model captures the persistence property of the Contourlet coefficients, and improves the segmentation accuracy, but this approach does not take the intrascale space neighborhood information into consideration, and can not eliminate the effect of speckle noise fundamentally. Otherwise, the method based on MRF captures the clustering of the coefficients. To this end, we propose a new method that fuses the segmentation results of above two algorithms by a fuzzy logic criterion. The fuzzy fusion method proposed in this paper is a nonlinear weighted logic operation which has the capacity of mixing the multi-source information together in accordance with their respective importance. So that the comprehensive performance in the two aspects the strengthening of space detail information and the precision of segmentation results of the ultimate integration image is improved.

Let H be the set of pixels, and $X = \{x_1, x_2, \dots, x_H\}$ the observed vectors, and the corresponding true classes for the pixels are $\Omega = \{w_{c1}, w_{c2}, \dots, w_{cH}\}$. The MAP method is to optimize the estimation of class labels $\hat{\Omega}$. From Bayesian theorem, the MAP labeling $\hat{\Omega}$ is found to be

$$\hat{\Omega} = \arg \max_{\Omega} \{p(X | \Omega) p(\Omega)\} \quad (1)$$

For the pixel x_g , is to find the class w_c that maximizes $p(w_c | x_g, w_{cg})$, Thus

$$\hat{w}_c = \arg \max_c \{p(w_c | x_g, w_{cg})\}, \forall g \quad (2)$$

where w_{cg} is the labeling on the pixels in a neighborhood surrounding pixel g . Assuming that the measurement vector x_g and the neighborhood labeling

$w_{\partial g}$ are independent.

$$p(w_c | x_g, w_{\partial g}) \propto p(x_g | w_c) p(w_c | w_{\partial g}) \quad (3)$$

where $p(x_g | w_c)$ denotes the probability of the central pixel x_g belonging to class w_c .

For each Contourlet coefficient, we define a binary hidden state S , which can take on the value 0 (insignificant coefficient) or 1 (significant coefficient). The marginal pdf of Contourlet coefficients is defined as

$$f(x_g) = \sum p(s=m) p(x_g | s=m) \quad (4)$$

where $p(x_g | s=m) \sim N(0, \sigma_{xm}^2)$ stands for a Gaussian distribution with a zero mean and variance σ_{xm}^2 . $p(s=m)$ is the probability mass function (pmf) and $p(s=0) + p(s=1) = 1$. Using this model, we can assume a prior probability function for $p(x_g | w_c)$. The measure of the pixel x_g with respect to the class w_c is

$$p(x_g | w_c) = \sum p(s=m) p(x_g | s=m) \quad (5)$$

For the σ_{xm} and $p(s=m)$ in the coefficient, we use the EM algorithm to estimate them.

$p(x_g | w_{\partial g})$ fuses the intrascale dependencies, and we employ the Gibbs distribution^[14] to find it out.

$$p(w_c | w_{\partial g}) = \frac{1}{z} \exp \{-U(w_c)\} \quad (6)$$

where z is a regular factor, and $U(w_c)$ is an energy function. The energy exponent is expressed as

$$U(w_c) = \sum_{\partial g} \beta [1 - \delta(w_c, w_{\partial g})] \quad (7)$$

where $\delta(w_c, w_{\partial g})$ is the Kroneker delta, $\beta > 0$ is a parameter with a value fixed by the user when applying the MRF technique. For an individual pixel, each algorithm provides as an output a membership degree for each of the considered classes. The set of these membership values is then modeled as a fuzzy set. To measure how fuzzy a fuzzy set, and thus estimate the ambiguity of the fuzzy set, we employ the measure of fuzziness based on the multiplicative class proposed by Pal and Bezdek in^[15], and we define the fuzzy measure function^[16] as follows

$$H_{\alpha QE}(u_F) = \frac{1}{N2^{-2\alpha}} \sum_{i=1}^n u_F(x_i)^\alpha (1 - u_F(x_i))^\alpha \quad (8)$$

The influence of parameter α : With α close to 0, all the fuzzy sets have approximately the same degree of fuzziness, and the measure is not sensitive to changes in u_F , whereas, the measure is highly selective, with the degree of fuzziness quickly decreasing when the fuzzy set differs from $u_F = 0.5$. Therefore, in this paper, we choose $\alpha = 0.5$ as a good trade off. For a C classes classification problem, we assume there are ml different classifiers are available. For a given pixel x_g , the output

of the classifier i is the set of numerical values:

$$\{u_i^1(x_g), u_i^2(x_g), \dots, u_i^j(x_g), \dots, u_i^C(x_g)\} \quad (9)$$

where $u_i^j(x_g) \in [0, 1]$ is the membership degree of the pixel x_g with respect to the class j according to the classifier i . The higher this value, the more likely it is that the pixel belongs to the class j . In any case, the set $\pi_i(x_g) = \{u_i^j(x_g), j=1, \dots, C\}$ can be considered as a fuzzy set.

As a conclusion, for every pixel, ml fuzzy sets are computed, one by each classifier. They constitute the input of the fusion process:

$$\{\pi_1(x_g), \pi_2(x_g), \dots, \pi_{ml}(x_g)\} \quad (10)$$

The probability of each pixel with respect to the class j is viewed as the fuzzy measurement. We weight each fuzzy set by

$$q_i = \frac{\sum_{k=0, k \neq i}^{ml} H_{\alpha QE}(\pi_k)}{(ml-1) \sum_{k=0}^{ml} H_{\alpha QE}(\pi_k)}, \text{ and } \sum_{i=0}^{ml} q_i = 1 \quad (11)$$

where $\alpha = 0.5$, $H_{\alpha QE}(\pi_k)$ is the fuzziness degree of the source, k and ml is the number of sources. When a source has a low fuzziness degree, q_i is close to 1, and it only slightly affects the corresponding fuzzy set. We can also use prior knowledge regarding the performance of each classifier, which is modeled for each classifier i and for each class j by a parameter f_i^j . For a given class j , if the results provided by the classifier are satisfactory, the parameter is set to 1 otherwise it is set to 0. Thus, the fusion rule is

$$u_f^j(x_g) = \max(\min(q_i u_i^j(x_g), f_i^j(x_g)), i \in [1, ml]) \quad (12)$$

Before this fusion step, the range of the fuzzy set is rescaled. This rescaled step is achieved by the following range stretching algorithm. For $\pi_i(x_g) = \{u_i^j(x_g), j=1, \dots, C\}$, compute

$$Ma = \max_{j,g} [u_i^j(x_g)], mi = \min_{j,g} [u_i^j(x_g)], \text{ For all } u_i^j(x_g),$$

compute

$$u_i^j(x_g) = \frac{u_i^j(x_g) - mi}{Ma - mi} \quad (13)$$

Substituting (7) into (3) and according to the fuzzy logic fusion operator, that is, (12), the ultimate formula is as follows:

$$g_{c_i}(x_g) = \max \left(\min q_{c_i} \left(-\frac{1}{2} \ln \left| \sum C_i \right| - \frac{1}{2} (x_g)^t \right. \right. \\ \left. \left. \times \sum C_i^{-1}(x_g) - \sum_{\partial g} \beta [1 - \delta(w_c, w_{\partial g})] \right), f_{c_i}(x_g) \right), \quad (14)$$

$$i = 1, 2, \dots, C$$

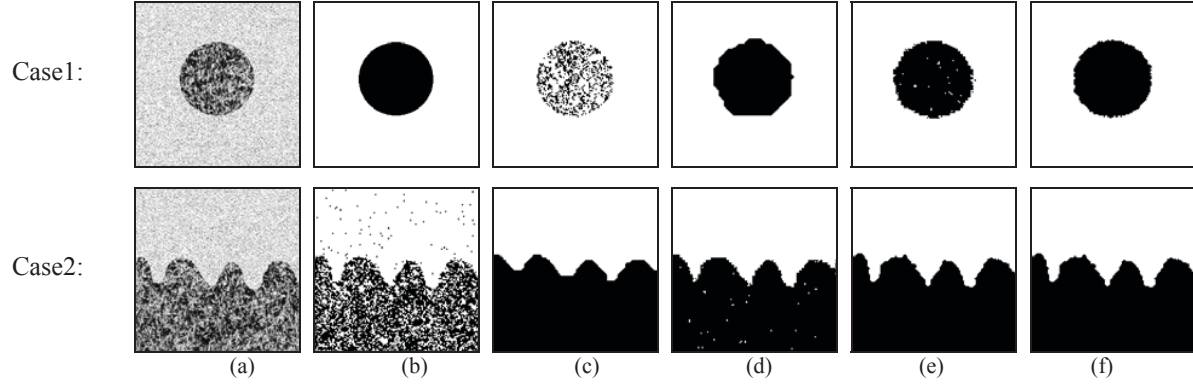


Fig.4 The segmentation results of synthetic texture image2:(a) synthetic texture image corrupted by multiplicative speckle noise of variance of 0.05; (b) manual segmentation; (c) Contourlet domain MRF Segmentation ; (d) wavelet domain HMT-HMF Segmentation; (e) Contourlet domain HMT segmentation; (f) proposed method.

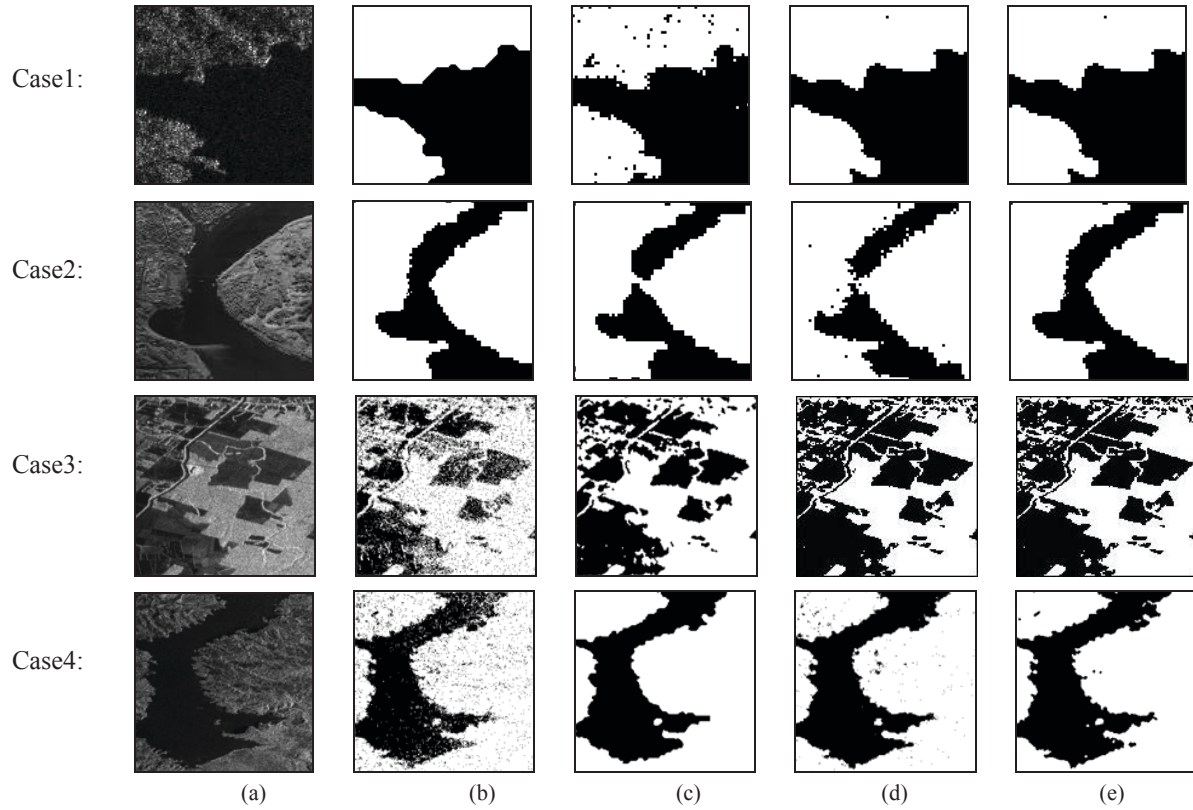


Fig.5 The segmentation results of real SAR image 4: (a) original image; (b) Contourlet domain MRF segmentation; (c) wavelet domain HMT-HMF segmentation; (d) Contourlet domain HMT segmentation; (e) proposed method.

Table 1 Segmentation Misclassification Ratios of different algorithms

Images	Case 1	Case 2
MRF in the Contourlet domain	0.1072	0.1874
HMT in the Contourlet domain	0.0189	0.0310
HMT-MRF in the wavelet domain	0.0174	0.0300
HMT-MRF in the Contourlet domain	0.0113	0.0210

IV. EXPERIMENTAL RESULTS AND ANALYSIS

For the Contourlet transform, we use the '9-7' biorthogonal filters for the multiscale decomposition stage and the 'PKVA' filter for the directional decomposition stage. To test the validity and popularity of our proposed algorithm, six groups of images are chosen. The first two are synthetic texture images corrupted by multiplicative speckle noise of variance of 0.05 and the others are real SAR images which are from Jet Propulsion Laboratory.

We begin with two synthetic texture images to

illustrate the performance of our algorithm, as shown in Fig.4, we can observe that both the methods based on the wavelet and Contourlet can give good segmentation results. However, compared with the method based on the wavelet, our method based on the Contourlet shows a better description of the contour. This is due to the disability of the separable wavelet, which is the extension of the one-dimensional wavelet.

The evaluation of two synthetic texture images segmentation results are shown in Table 1. The segmentation of synthetic texture images can only show the effectiveness of the proposed algorithm, but can not show its extensive application. So we choose the real SAR images for test.

In fig.5, for comparison, the contourlet domain HMT method, MRF method and wavelet domain HMT-MRF method are also presented. In case 1, the two textures are land and sea, respectively. From case 1, (a), we can see that some regions in the land part have the same statistical property as in the sea, so the Contourlet domain MRF method which only considers neighbors and the HMT method which only captures the persistence of Contourlet coefficients can not get accurate segmentation, leading to the mistake. Our method which takes advantage of the strengths of the two methods fuses the clustering and persistence of Contourlet coefficients, effectively suppresses the influence of speckles and achieves superior contour representation and excellent visual performance. Case 2 is the Ku band airborne SAR image whose size is 128×128 with $ENL=3.2203$; Case 3 and case 4 are real airborne SAR images which are of the L band and whose size are 512×512 with $ENL=2.8406$ and $ENL=1.6783$, respectively. Similar behaviors are also observed in the following SAR images. The same conclusions can also be obtained from Case 2~4, which approves the validity of our method.

V. CONCLUSIONS

In this paper we presented a new SAR images segmentation algorithm based on HMT-MRF fuzzy fusion in the Contourlet domain. This algorithm extends the Markov random field (MRF) to the Contourlet domain, and characterizes the persistence and clustering property of Contourlet subbands by the HMT and MRF model, respectively. Then we establish a new HMT-MRF fusion model by introducing the fuzzy logic operator, and improve the estimation accuracy by adopting the variable local smoothness in the Gibbs equation. On the basis of all above, we deduced the MAP segmentation formula for the new model. We applied the proposed algorithm to synthetic texture images and real SAR images. The experimental results and analysis show that the proposed algorithm effectively suppresses the effect of noise and provides superior contour representation and excellent visual performance.

ACKNOWLEDGMENT

This work is supported by the National Natural Science Foundation of China (No.60872137), the National Defence Foundation of China (No.9140A01060408DZ0104), and by the Aviation Science Foundation of China (20080181002).

REFERENCES

- [1] B., Dalila and P., Wojciech.: Unsupervised Statistical Segmentation of Nonstationary Images Using Triplet Markov Fields, *IEEE Trans. PAMI* 29(8) (2007) 1367-1378.
- [2] Wu, Yan, Wang, Xia, Liao, Guisheng.: SAR Images Despeckling via Bayesian Fuzzy Shrinkage Based on Stationary Wavelet Transform, *Applied and Numerical Harmonic Analysis*, December 2006, pp.407-418.
- [3] Wu, Yan, Wang, Xia, Liao, Guisheng.: SAR images despeckling based on wavelet and hidden Markov mixture model, *Chinese Journal of Radio Science* 22(2) (2006) 244-250.
- [4] V., Venkatachalam, H., Choi.: Multiscale SAR image segmentation using wavelet-domain hidden Markov tree model, *SPIE* 3497 (1998) 141-151.
- [5] H., Choi, R. G., Baraniuk.: Multiscale image segmentation using wavelet-domain hidden Markov models, *IEEE Trans. Image Process.* 10(9) (2001) 1309-1321.
- [6] A.David, Clausi, Xue, Bing.: Comparing Cooccurrence Probabilities and Markov Random Fields for Texture Analysis of SAR, Sea Ice Imagery *IEEE Trans. Geo. Rem. Sen.* 42(1) (2004) 215-228.
- [7] Deng Huawu, D. A., Clausi.: Unsupervised segmentation of synthetic aperture radar sea ice imagery using a novel Markov random field model, *IEEE Trans. on GRS* 43(3) (2005) 528-538.
- [8] O., Lankoande, M. M., Hayat, Balu. Santhanam.: Segmentation of SAR images based on Markov random field model, 2005 IEEE International Conference on System, Man and Cybernetics, United States, 3 (2005) 2956-2961.
- [9] Xie, Hua, L. E. Pierce, F. T., Laby.: Speckle Reduction using Wavelet Denoising and Markov Random Field Modeling, *IEEE Trans. on GRS*, 40(10) (2002) 2196-2212.
- [10] M.N.Do., M. Vetterli.: the contourlet transform: an efficient directional multiresolution image representation, *IEEE Trans. on Image Process.* 14 (12) (2005) 2091 - 2106.
- [11] D.Y. Po, Duncan and M.N.Do.: directional multiscale modeling of images using the Contourlet transform, *IEEE Trans. on Image Processing* 15(6) (2006) 1610-1620.
- [12] A.L.da., J.Zhou Cunha, M.N.Do.: the nonsubsampled Contourlet transform: theory, design and application, *IEEE Trans. Image Processing* 15(10) (2006) 3089-3101.
- [13] Sha, Yuheng, Jiao, Licheng.: unsupervised image segmentation using Contourlet domain hidden Markov tree model, *ICIAR* (2005) LNCS3656, 32-39.
- [14] C.A., Bouman, M. Shapiro.: multiscale random field model for Bayesian image segmentation, *IEEE Trans. on Image Processing* 3(2) (1994) 162-177.
- [15] N.R. Pal and J.C. Bezdek.: Measuring fuzzy uncertainty, *IEEE Trans. Fuzzy Syst.* 2(2) (1994) 107-118.
- [16] Fauvel, Mathieu, Chanussot, Jocelyn.: Decision Fusion for the Classification of Urban Remote Sensing Images, *IEEE Trans. on Geoscience and Remote Sensing* 44(10) (2006) 2828-2838.